ELSEVIER

Journal of Alloys and Compounds 253–254 (1997) 648–651

Journal of ALLOYS AND COMPOUNDS

Influence of preparation methods of non-stoichiometric hydrogen-absorbing alloys on the performance of nickel–metal hydride secondary batteries

N. Higashiyama*, Y. Matsuura, H. Nakamura, M. Kimoto, M. Nogami, I. Yonezu, K. Nishio

Sanyo Electric Co. Ltd., New Materials Research Center, 1-18-13, Hashiridani, Hirakata City, Osaka 573, Japan

Abstract

$Mm(Ni_{3.8}Al_{0.2}Mn_{0.6})_{(x-0.4)/4.6}Co_{0.4}$ alloys with stoichiometry $5.0<x<5.8$ were prepared through a rapid quenching process. Their microstructural and electrochemical characteristics were examined with regard to discharge capacity and durability of the negative electrode in a Ni–metal hydride (MH) battery. These multi-component alloys exhibited a high electrochemical reactivity and their discharge capacities were dominated by the stoichiometry x. The charge–discharge cycling stability was influenced by both stoichiometry and microstructure. The non-stoichiometry brought microstructural heterogeneity. However, the rapid quenching process homogenized it effectively and enhanced the cycle performance. Consequently, a capacity of 310 mA h g^{-1} and a durability of up to 500 cycles were obtained in rapidly quenched $Mm(Ni_{3.8}Al_{0.2}Mn_{0.6})_{(x-0.4)/4.6}Co_{0.4}$ ($x=5.2$).

Keywords: Hydrogen-absorbing alloy; Stoichiometry; Nickel–metal hydride battery; Rapid quenching

1. Introduction

It is widely known that the stoichiometry x of rare earth–nickel type alloys such as $LaNi_x$, significantly affects their hydrogen-absorbing properties [1]. The influence of x on the electrochemical properties of multi-component AB_x type hydrogen-absorbing alloys for battery use has also been investigated [2,3]. Nogami et al. reported that some non-stoichiometric alloys with compositions of [$Mm(Ni–Co–Al–Mn)_x$: $4.5\leq x\leq 4.8$] showed approximately 10% higher discharge capacity than the stoichiometric alloy [2].

Notten et al. have studied on $La(Ni–Cu)_x$ alloys to enhance charge–discharge cycle performance [4,5]. These studies were aimed at the development of Co-free alloys which would contribute to cost reduction. Co has been reported [6] to be an indispensable element to enhance the charge–discharge cycle performance. Notten et al. found that increasing the stoichiometry beyond $x=5$ led to a higher charge–discharge cycle durability, although the substitution of Cu for Ni formed an enriched phase on the alloy surface which reduced the electrochemical catalysis [7]. The surface of a rare earth–nickel type alloy is considered to be covered with Ni or Co-enriched layers which provide a high electrochemical reactivity [8,9].

On the other hand, the non-stoichiometry in the rare earth–nickel alloys is reported to promote a segregation or precipitation of MmNi, Mn and Al–Ni alloys [10,11] which reduce cycle performance due to their smaller durability against oxidization. In order to suppress the segregation of the alloy, a rapid quenching process has been applied to AB_2 and AB_5 type hydrogen-absorbing alloys [12,13].

In this work, we investigate the effects of the rapid quenching and non-stoichiometry on the electrochemical discharge capacity and durability of $Mm(Ni_{3.8}Al_{0.2}Mn_{0.6})_{(x-0.4)/4.6}Co_{0.4}$ ($5.0\leq x\leq 5.8$) alloys which are candidates for use as negative-electrode materials for commercial Ni–MH batteries.

2. Experimental details

Mixtures of raw materials with compositions of $Mm(Ni_{3.8}Al_{0.2}Mn_{0.6})_{(x-0.4)/4.6}Co_{0.4}(5.0\leq x\leq 5.8)$ were melted using an induction furnace, followed by a rapid quenching process of strip-casting on a rotating copper roll. Samples with the corresponding compositions were also prepared using induction melting followed by casting into a mold. Mischmetal including 50 wt% Ce was employed.

Both series of samples were crushed and ground into a powder which was sieved through a 200–500 mesh and used for the metal hydride (MH) electrode preparation.

*Corresponding author.

0925-8388/97/$17.00
PII S0925-8388(96)03076-9

Powders denoting a grain mix of approximately 100 μm were used for the measurement of Pressure–Composition (P–C) isotherms of approximately 50 μm for X-ray powder diffraction (XRD) measurements.

The electrodes for measuring electrochemical properties were fabricated by mixing the sieved alloy powder with carbonyl–nickel powder and polytetrafluoroethylene, followed by shaping the mixture wrapped with a nickel net into pellets. The electrodes were tested at 298 K in an electrochemical half cell with a sintered nickel electrode as a counter electrode, a half-charged sintered nickel electrode [14] as the reference electrode and a 30 wt% KOH solution as the electrolyte.

The electrochemical reactivity of the alloy was evaluated by using the initial discharge curve. After the electrode was charged at 50 mA g^{-1} for 8 h, the discharge capacity was measured at 200 mA g^{-1} (capacity C_{200}) and 50 mA g^{-1} (capacity C_{50}) until the potential of the MH electrode reached −0.95 V with respect to the reference electrode. The ratio of $C_{200}/(C_{200}+C_{50})$ was employed for evaluating the reactivity. A charge–discharge cycle was conducted at 50 mA g^{-1} until the maximum capacity of the MH electrode was observed.

The sealed test cells of commercial AA size were fabricated with an alloy powder-pasted negative electrode and a sintered nickel-type positive electrode having a capacity of 1000 mA h. A charge–discharge cycle test at 1500 mA while discharging down to 1.0 V of cell voltage and charging in a $-\Delta V$ method was conducted until the capacity of the battery decreased below 500 mA h.

The crystallography and microstructure of the alloys were examined by X-ray powder diffractometry (XRD) and electron probe microanalysis (EPMA). The alloy powder was removed from the electrode in the cell after 100 cycles and its oxygen concentration was determined by the infrared absorption method using a LECO oxygen determinator, Model RQ-416DR.

3. Results and discussion

3.1. Discharge capacity and electrochemical reactivity

Absorption P–C isotherms at 313 K of the rapidly quenched and conventional cast alloys are shown in Fig. 1. The rapid quenching process flattened the plateau region compared to the conventional cast process, especially for the stoichiometry $5.0 \leq x \leq 5.4$, without reducing the maximum hydrogen content. The results suggest that the rapid quenching process gives a more homogeneous compositional distribution than the conventional cast process.

The electrochemical parameters are listed in Table 1, which were obtained from the electrochemical half cells. Both the rapidly quenched and conventional cast alloys exhibited almost the same discharge capacity and electrochemical reactivity. The maximum discharge capacity

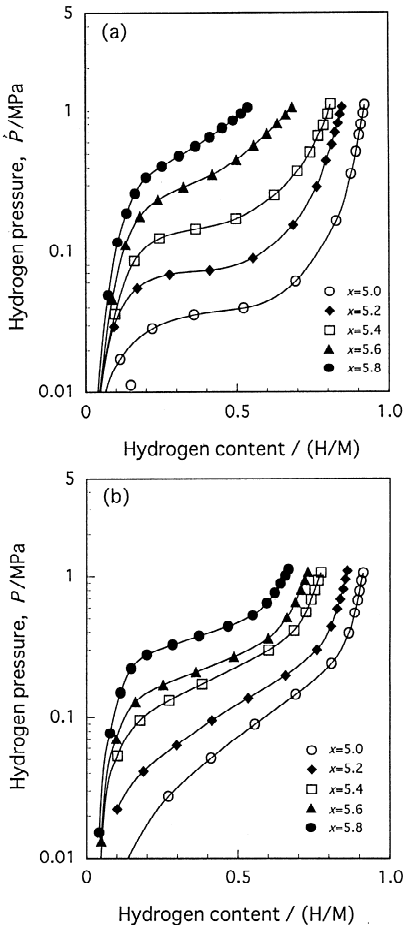

Fig. 1. P–C isotherms at 313 K of: (a) rapidly quenched, and (b) conventional cast alloys.

decreased with increasing x in both alloys. This electrochemical behaviour is in accordance with the results from the P–C isotherm measurements which show that the hydrogen storage capacity at constant hydrogen pressure decreases with increasing x. The electrochemical reactivity for $C_{200}/(C_{200}+C_{50})$ exceeds 90% for most of the rapidly quenched alloys.

These results suggest that their discharge capacity is dominated by the stoichiometry.

3.2. Electrochemical cycle stability

The cycle stability of the sealed test cell $S(n)$ listed in Table 1 is the ratio of the discharge capacity at cycle number n to the designed capacity (1000 mA h). The decay in discharge capacity was stopped by the rapid quenching process. In particular, the rapidly quenched alloys with the stoichiometries $x=5.2$ and $x=5.4$, revealed a much higher cycle stability than the other alloys, remaining at approximately 80% of the designed capacity even after 500 cycles, as expressed in S(500).

The increasing amount of oxygen concentration, $C(n)$, of the alloy during the cycle is also summarized in Table 1. A

Table 1
Electrochemical features and parameters of sealed nickel–metal hydride batteries

	AB_x	Discharge capacity (mA h g^{-1})	Reactivity $C_{200}/(C_{200}+C_{50})$ (%)	Stability			Oxidation			Particle size $D(100)$ (%)
				$S(100)$ (%)	$S(300)$ (%)	$S(500)$ (%)	$C(100)$ (wt%)	$C(300)$ (wt%)	$C(500)$ (wt%)	
Rapidly quenched	$AB_{5.0}$	335	91	89.5	–	–	4.05	–	–	19
	$AB_{5.2}$	310	88	98.0	93.8	79.5	1.81	4.01	5.85	51
	$AB_{5.4}$	293	89	97.1	92.0	78.9	1.64	3.37	5.67	79
	$AB_{5.6}$	242	90	85.7	67.5	–	3.34	6.62	–	18
	$AB_{5.8}$	212	90	70.7	–	–	4.36	–	–	37
Conventional cast	$AB_{5.0}$	333	94	87.7	–	–	5.38	–	–	18
	$AB_{5.2}$	315	95	92.2	60.3	–	2.28	6.39	–	19
	$AB_{5.4}$	297	95	85.5	–	–	4.58	–	–	19
	$AB_{5.6}$	270	96	88.3	55.3	–	2.82	6.31	–	15
	$AB_{5.8}$	254	96	76.2	–	–	4.42	–	–	17

comparison of $S(n)$ and $C(n)$ indicates that the discharge capacity decreases with increasing oxygen concentration. This suggests that the oxidization of the alloy shortens the cycle life of the battery.

The relative average particle size diameter of the alloys after 100 cycles, which is a ratio of average particle size diameter after 100 cycles to the initial one, is shown as $D(100)$ in Table 1. Larger particle sizes were observed in the rapidly quenched alloys than in the conventional cast alloys. In particular, the particle sizes for the rapidly quenched alloys of stoichiometry $x=5.2$ and $x=5.4$ which exhibited high cycle stability and low oxygen concentration, were apparently larger.

The charge–discharge cycles can generate cracks in the alloy powder which reduce its grain size and increase the rate of oxidization due to the increasing surface area [15–18]. Therefore, the pulverizing behaviour of the alloys should be regarded as an important factor dominating the cycle stability. Notten et al. reported that the cycle stability of AB_x alloys increased with increasing x [5,15,16,19] because of a reduced pulverization due to the smaller difference in lattice expansion between the α and β phase. ln the results obtained here, however, the cycle stability decreased in spite of the fact that x became greater than 5.4. Therefore, there must be other factors responsible for the pulverizing of the alloys.

3.3. Microstructure and its influence on the electrochemical behaviour

Fig. 2 shows XRD patterns of the rapidly quenched and conventional cast alloys. All peaks except the dot-marked ones at 44° were assigned to the hexagonal $CaCu_5$ type structure. The dot-marked peaks could be assigned to Mn or Ni metal or the related solid solution. The peak at 44° appeared only in conventional cast alloys with the stoichiometry $x \geq 5.4$ and grew with increasing x. In the rapidly quenched alloys, however, no peak was observed at $2\theta=44°$, even at the stoichiometry $x=5.8$. This means that the rapid quenching process effectively homogenized the microstructure and brought about single-phase compounds. On the other hand, the broadening of (002) reflection at 44.7° with increasing x indicated an anisotropic lattice distortion. This result suggests that an increase of x promotes microstructural heterogeneity and pulverization of the rapidly quenched alloys particularly in the case of $x>5.4$.

Fig. 3 shows typical X-ray images of Mn for the rapidly quenched and conventional cast-alloy samples. Segregation of Mn was apparently observed in the conventional cast alloys and even in the rapidly quenched alloys, while the segregating area of the conventional cast alloys was dispersed through the rapid quenching process. This change in the microstructure is considered to be one factor for the improved cycle performance in the rapidly

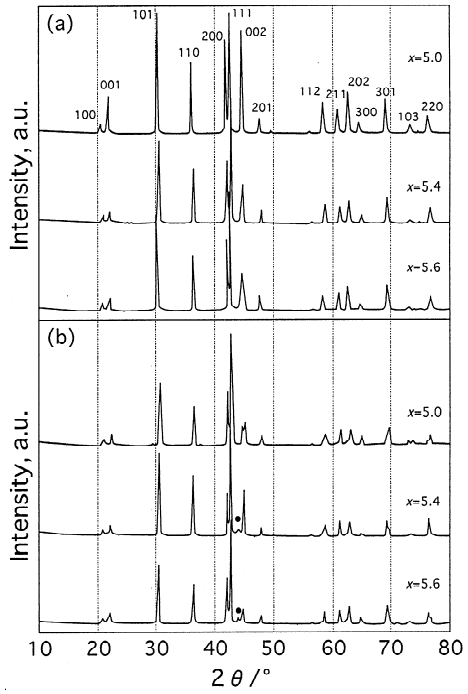

Fig. 2. X-ray powder diffraction patterns for: (a) rapidly quenched, and (b) conventional cast alloys.

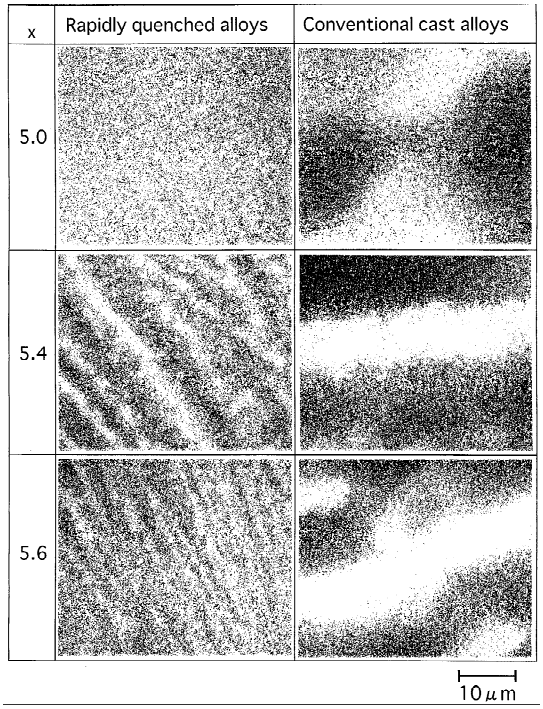

Fig. 3. X-ray images (Mn) of rapidly quenched and conventional cast alloys.

quenched alloys. Segregation of manganese seems to become stronger with increasing x, even in the rapidly quenched alloys. This could be the reason why the stability $S(100)$ in Table 1 decreased above $x=5.4$.

4. Conclusions

$Mm(Ni_{3.8}Al_{0.2}Mn_{0.6})_{(x-0.4)/4.6}Co_{0.4}$ alloys with stoichiometries $5.0 \leq x \leq 5.8$ were prepared through a rapid quenching process. Their microstructural and electrochemical characteristics were examined in regard to discharge capacity and durability of the negative electrode in Ni–metal hydride (MH) batteries. The conclusions are as follows.

1. The discharge capacity is dominated by the stoichiometry.
2. The charge–discharge cycle stability is dependent on both stoichiometry and microstructural homogeneity of the alloys.
3. Rapid quenching effectively homogenizes the microstructure of the alloys and improves the durability.
4. Consequently, a capacity of 310 mA h g^{-1} and a durability of up to 500 cycles were obtained in rapidly quenched $Mm(Ni_{3.8}Al_{0.2}Mn_{0.6})_{(x-0.4)/4.6}Co_{0.4}$ alloys with $x=5.2$.

Rapidly quenched $Mm(Ni_{3.8}Al_{0.2}Mn_{0.6})_{(x-0.4)/4.6}Co_{0.4}$ alloys with $(5.2 \leq x \leq 5.4)$ would be candidates for negative electrode materials in commercial Ni–MH batteries. On the basis of the effects of non-stoichiometry and rapid quenching novel hydrogen-absorbing alloys with lower Co content can be developed for battery use.

References

[1] K.H.J. Buschow and H.H. van Mal, *J. Less-Common Met., 29* (1972) 203.
[2] M. Nogami, M. Tadokoro, M. Kimoto, Y. Chikano, T. Ise and N. Furukawa, *Denki Kagaku, 61* (1993) 1088.
[3] Y. Fukumoto, M. Miyamoto, M. Matsuoka and C. Iwakura, *Electrochimica Acta, 7* (1995) 845.
[4] P.H.L. Notten, R.E.F. Einerhand and J.L.C. Daams, *J. Alloys Comp., 210* (1994) 221.
[5] P.H.L. Notten, J.L.C. Daams and R.E.F. Einerhand, *J. AIIoys Comp., 210* (1994) 233.
[6] J.R. van Beek, H.C. Donkersloot, J.J.G. Willems, *Proc. 14th Intern. Power Sources, 1984*, p. 317.
[7] F. Meli, A. Züttel and L. Schlapbach, *J. Alloys Comp., 202* (1993) 81.
[8] F. Meli, T. Sakai, A. Züttel and L. Schlapbach, *J. Alloys Comp., 221* (1995) 284.
[9] I. Yonezu and M. Nogami, *Proc. 7th Canadian Hydrogen Workshop, Quebec, Canada, 1995*, p. 171.
[10] T. Sakai, H. Yoshinaga, H. Miyamura, N. Kuriyama and H. Ishikawa, *J. Alloys Comp., 180* (1992) 37.
[11] P.H.L. Notten and P. Hokkeling, *J. Electrochem. Soc., 138* (1991) 1877.
[12] S. Fujiwara, B. Kurishinann, Y. Moriwaki and I. Matsumoto, *The Electrochem. Soc., Proc., 94(27)* (1994) 172.
[13] M. Kanda, H. Hasebe, Y. Isozaki and S. Inada, *18th Electrochem. Soc. Meeting., Extend Abstracts, 94(2)* (1994) 71.
[14] D.E. Holl, *J. Electrochem. Soc., 130* (1983) 317.
[15] P.H.L. Notten, R.E.F. Einerhand and J.L.C. Daams, *J. Alloys Comp., 210* (1994) 216.
[16] P.H.L. Notten, R.E.F. Einerhand and J.L.C. Daams, *J. Alloys Comp., 231* (1995) 604.
[17] J.J.G. Willems, *Philips J. Res., Suppl. I., 39* (1984) 1.
[18] J.J.G. Willems and K.H.J. Buschow, *J. Less-Common Met., 129* (1987) 13.
[19] P.H.L. Notten, J.L.C. Daams and R.E.F. Einerhand, *Ber. Bunsenges. Phys. Chem., 96* (1992) 656.